Stress, strain and magnetostriction in epitaxial films

2002 J. Phys.: Condens. Matter 14 4165

(http://iopscience.iop.org/0953-8984/14/16/308)

INSTITUTE OF PHYSICS PUBLISHING JOURNAL OF PHYSICS: CONDENSED MATTER

J. Phys.: Condens. Matter **14** (2002) 4165–4176 PII: S0953-8984(02)29080-3

Stress, strain and magnetostriction in epitaxial films

D Sander[1], **S Ouazi, A Enders, Th Gutjahr-Löser, V S Stepanyuk, D I Bazhanov and J Kirschner**

Max-Planck-Institut für Mikrostrukturphysik, Weinberg 2, D-06120 Halle/Saale, Germany

E-mail: sander@mpi-halle.de

Received 29 September 2001, in final form 13 November 2001
Published 11 April 2002
Online at stacks.iop.org/JPhysCM/14/4165

Abstract

The application of the cantilever bending technique to stress measurements at surfaces and in epitaxial films is elucidated. The role of elastic anisotropy in quantitative cantilever curvature analysis is discussed. The stress in Co monolayers is measured *during* epitaxial growth on Cu(001). The Co-induced stress is found to oscillate with a period of one atomic layer. Simultaneous stress and medium-energy electron diffraction identify maximum stress for filled Co layers. Strain relaxation in Co islands leads to the reduced stress contribution of 2.9 GPa in the partially filled top layer as compared to 3.4 GPa for the filled layers. The cantilever technique is also applied to measure magnetoelastic properties of nanometre thin epitaxial films. Our measurements reveal that the magnetoelastic-coupling coefficients in epitaxial Fe, Co and Ni films differ from the respective bulk values. It is proposed that the epitaxial misfit strain is of key importance for this peculiar magnetostrictive behaviour of ultrathin films.

(Some figures in this article are in colour only in the electronic version)

1. Introduction

Almost all electronic devices rely on the proper functioning of often quite complex film and multilayer structures that are deposited on a substrate. The deposition of a film on a substrate is generally connected with the build-up of mechanical stress and consequently the elastic energy of the system increases accordingly. Due to its possible detrimental effect on device performance, experimental investigations of film stress have a long tradition and many reviews are devoted to this topic [1–6].

However, it is important to realize that current electronic and magnetoelectronic devices work with film structures where the single-layer thickness is only a few atomic layers [7]. Therefore the venerable stress measurement of thin films, where *thin* means in the micrometre

[1] Corresponding author.

range, has to be boosted in sensitivity by at least three orders of magnitude to investigate stress in (sub)nanometre *ultrathin* films.

This paper describes a stress measurement technique that gives subatomic layer sensitivity. This high sensitivity allows investigation of the correlation between atomic rearrangement in a monolayer and the resulting stress. As an example, we present measurements of stress oscillations during film growth, which show a 1 ML period. We ascribe the stress oscillations to subtle atomic relaxations in monolayer islands during growth.

In this work we concentrate on epitaxially well defined and characterized atomic layers, deposited on single crystal surfaces. These epitaxial systems make a connection between experimental and first principles calculations on stress in atomic layers and at surfaces feasible [8–13], and we performed *ab initio* based calculations to identify the atomic origin of the measured stress oscillations.

The high sensitivity of the cantilever bending technique is employed to measure magnetostrictive stresses in ferromagnetic monolayers. Magnetoelastic-coupling coefficients in epitaxial atomic layers are determined from the magnetization-induced bending of the film–substrate composite. These stresses are of the order of a only a few MPas, three orders of magnitude smaller than a typical epitaxial misfit stress in the order of GPas. Our results indicate the decisive role of film strain for the measured non-bulk-like magnetoelastic behaviour of nanometre films. This result is of utmost importance for understanding and tuning magnetic anisotropy in thin films [14].

Our experimental set-up to measure stress with submonolayer sensitivity is presented in section 2. The effect of elastic anisotropy and sample clamping on the curvature analysis is discussed in section 3. Stress oscillations during film growth are presented in section 4. The application of the curvature technique to measure the magnetostrictive properties of ferromagnetic monolayers follows in section 5.

2. Experimental set-up

The idea of cantilever stress measurements is very simple: a thin rectangular substrate is clamped at one end along its width to a sample manipulator, with the opposite end remaining free. Any change in stress on one of the surfaces of the substrate will induce a curvature of the substrate. For the measurements that we perform, the stress imbalance between the two surfaces can be due to adsorption, film growth or magnetization of the deposited film. Thus, a measurement of the change in substrate curvature allows a direct and quantitative analysis of adsorbate-induced changes of surface stress, of thickness-integrated film stress, or of the magnetoelastic-coupling coefficients of ferromagnetic layers. A detailed analysis of the curvature technique can be found in [14–20].

Many techniques have been applied to detect the substrate curvature [14, 17], here we describe a simple optical deflection set-up, shown in figure 1.

The stress-induced curvature of the single crystalline substrate is detected by reflecting two laser beams from the substrate surface to two position-sensitive detectors. Two detector signals are recorded, which are proportional to the change in slope of the substrate at the positions, where the spots are reflected. We calculate the difference between the two signals, and thus we obtain the change in slope of the substrate over the spot distance, which is to a very good approximation proportional to the curvature $\kappa = 1/R$. For a substrate thickness of order 0.1 mm, typical radii of curvature R are of the order 100 m for epitaxial film stress in the GPa range, and can be as large as 100 km for magnetoelastic stress, which is often in the MPa range. From the measured change of curvature $\Delta\kappa$, the corresponding change in surface stress $\Delta\tau_s$ is calculated from the Stoney equation: $\Delta\tau_s = Yt^2\Delta\kappa/(6(1-\nu))$, where the substrate thickness is given by t. For the measurement of a film stress τ_F with film thickness t_F, $\tau_s = \tau_F t_F$.

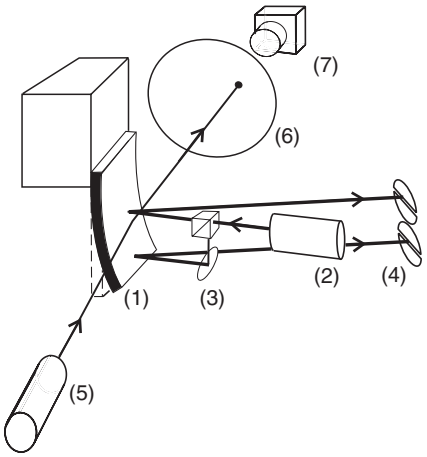

Figure 1. Two-beam curvature measurement with simultaneous MEED measurement. (1) Sample, (2) laser, (3) beamsplitter and mirror, (4) two position-sensitive detectors, (5) electron gun, (6) LEED screen, (7) CCD camera.

Note that only the elastic properties of the substrate are needed in the analysis, and knowledge of the elastic properties of the monolayer-thin film is not required. The elastic properties of crystals are highly anisotropic, and proper tensor transformations have to be applied to use the appropriate values of Young's modulus Y, and Poisson's ratio ν, for the exposed substrate surface and orientation [14,21]. The analysis is also affected by the clamping of the substrate and these issues are discussed next.

3. Elastic anisotropy and sample clamping

The elastic properties of all elements with the exception of W are highly anisotropic. For example, for Fe the magnitude of Young's modulus Y, which is given by the elastic compliance $1/s_{11}$, varies by almost a factor of 2 for different orientations within the (100)-plane. Fe is stiff along the [110] direction ($Y = 218$ GPa), and softer along [100] ($Y = 131$ GPa), and the Poisson ratio also varies in magnitude and even in sign. The elastic anisotropy of Fe, Si and Mo in the (100)-plane is depicted by the polar plots of figure 2.

The anisotropy presented in these plots confirm that proper tensor transformations are necessary for a quantitative analysis of the curvature measurement. For cubic elements the respective transformations are

$$\text{cubic: } 1/Y' = s'_{11} = s_{11} - 2(s_{11} - s_{12} - \tfrac{1}{2}s_{44})(l_1^2 l_2^2 + l_1^2 l_3^2 + l_2^2 l_3^2) \tag{1}$$

$$\text{cubic: } \nu' = -\frac{s'_{12}}{s'_{11}} = -\frac{s_{12} + (s_{11} - s_{12} - \frac{1}{2}s_{44})(l_1^2 m_1^2 + l_2^2 m_2^2 + l_3^2 m_3^2)}{s_{11} - 2(s_{11} - s_{12} - \frac{1}{2}s_{44})(l_1^2 l_2^2 + l_1^2 l_3^2 + l_2^2 l_3^2)} \tag{2}$$

where the directions with respect to the cubic axes are denoted by the direction cosines l_i and m_i. The direction cosines l_i and m_i are given by the projections of the unit vectors e'_1 and e'_2, respectively, of the transformed coordinate system onto the cubic axes i [14, 18]. Thus, the proper values for Y and ν in the Stoney equation can be calculated. Note that for cubic elements the biaxial modulus $Y/(1 - \nu)$ is isotropic within the (100) plane, see right-hand column in figure 2, and that both Y and ν are isotropic in the (111) plane.

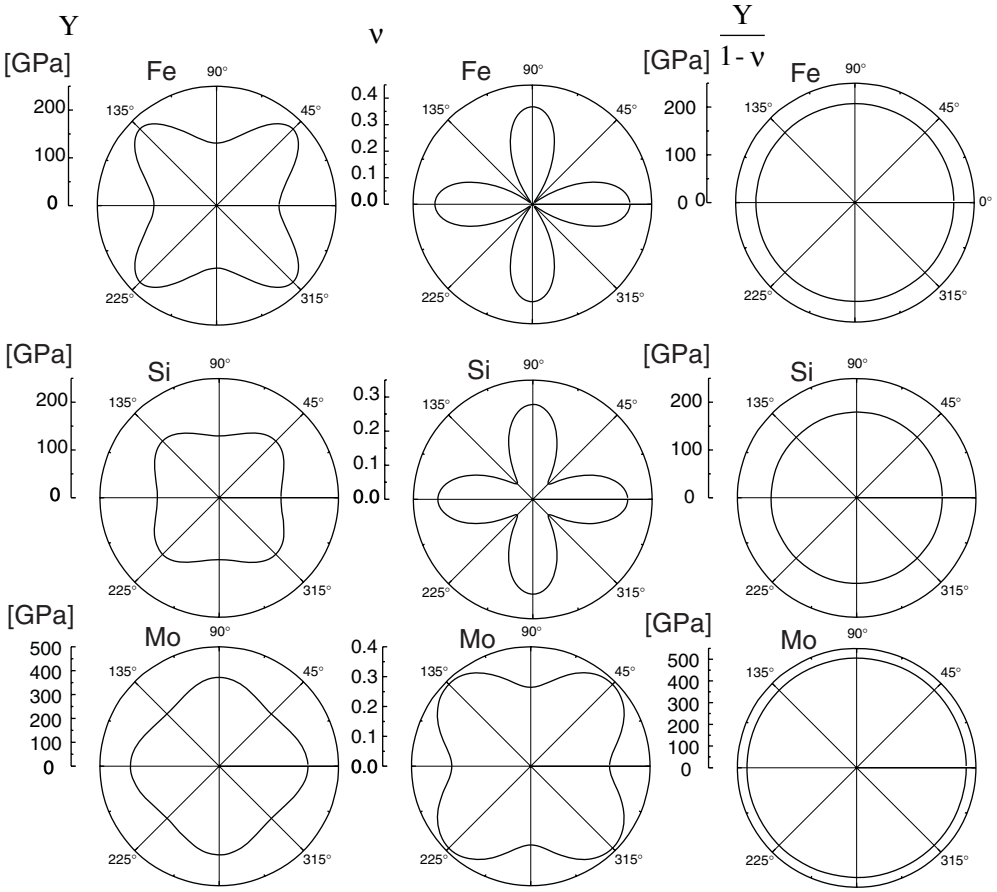

Figure 2. Polar plots of (a, d, g) Young's modulus Y, (b, e, h) Poisson's ratio ν and (c, f, i) biaxial modulus $Y/(1-\nu)$, for the cubic elements: (a)–(c) Fe, (d)–(f) Si and (g)–(i) Mo. All polar plots are for the (100)-surface orientation, with the cubic axis ⟨100⟩ running horizontally.

In general, the growth of a film, or the adsorption of a gas, or the change of the in-plane magnetization direction of a ferromagnetic monolayer induces a biaxial change in stress. Consequently, the substrate is forced to curve along its length *and* along its width. Therefore, a clamping along the width will always have an impact on the curvature along the width. In the extreme case of hindered curvature along the width and biaxial stress, the expression of the Stoney equation has to be modified to $\Delta\tau_s = Yt^2\Delta\kappa/(6(1-\nu^2))$. In experiments, this case is approximately encountered for substrates with a small (<0.2) length-to-width ratio. A detailed finite-element-method analysis of the bending of a clamped substrate has been performed by Dahmen *et al* [18], and one result is presented in figure 3. The authors use the following:

$$\tau t_F = \frac{Yt^2\kappa}{6(1-\nu)(1+(2-D)\nu)} \tag{3}$$

to express the impact of the clamping along the width by introducing the dimensionality parameter D.

The results of the calculations in figure 3 show that a measurement of the curvature leads to much smaller corrections as compared to deflection measurements. For curvature

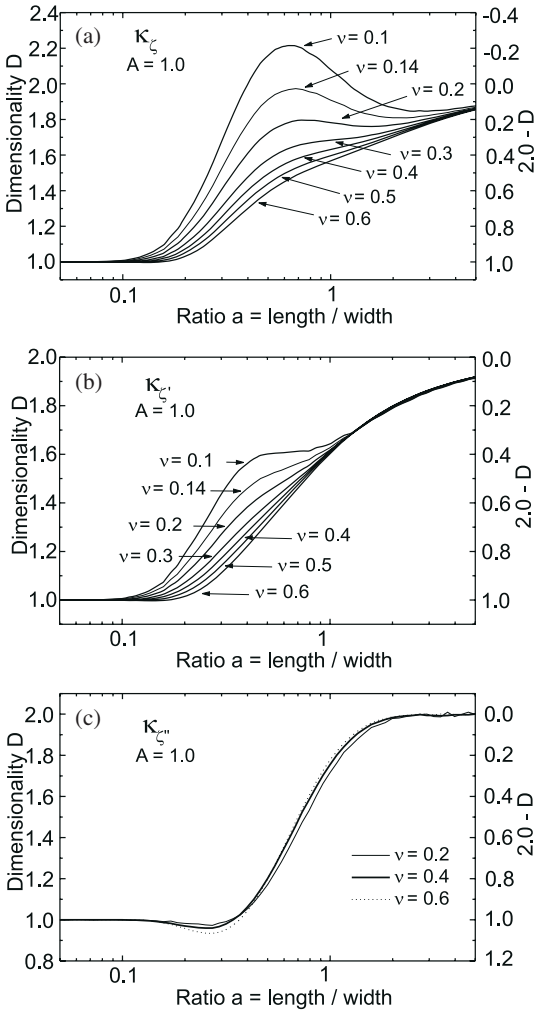

Figure 3. Dependence of the dimensionality D of the bending on the length-to-width ratio a of an elastically isotropic sample, $A = 1$, and different Poisson ratios ν [18]. (a) The curvature κ_ζ calculated from the sample deflection influenced most by the clamping as compared to the curvature κ'_ζ determined from the sample slope. (b) A direct measurement of the curvature κ''_ζ is influenced the least by the clamping as indicated by $D \approx 2$ for a moderate value of $a = 2$. From [18], with kind permission of the authors.

measurements, a moderate length-to-width ratio of 2 already leads to negligible corrections as indicated by the dimensionality $D = 2$.

In conclusion, the two-beam curvature measurement employed on our samples, which are 15 mm long and 2.5 mm wide, is a very good approximation of a free two-dimensional bending, and quantitative stress measurements are feasible and are presented next.

4. Stress oscillations during film growth

An oscillatory variation of the in-plane lattice spacing of epitaxial islands has been observed by diffraction techniques for semiconductor [22] and metal growth [23, 24]. However, the respective signature of oscillating film forces has not been reported up to now. A recent

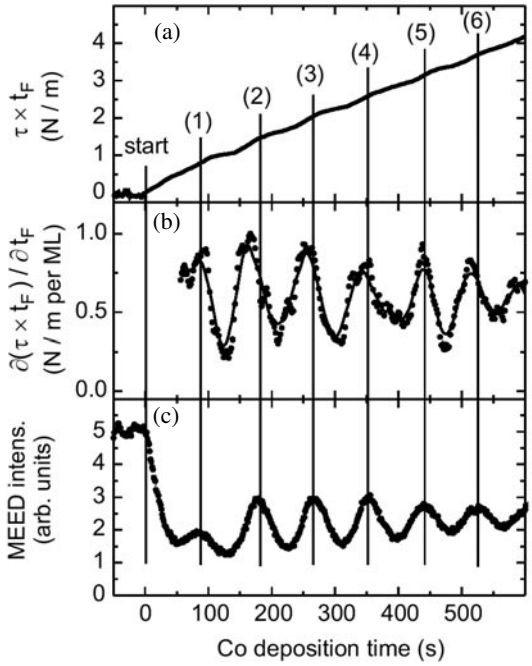

Figure 4. Stress and simultaneous MEED intensity measurements during the growth of Co on Cu(001) at 300 K. (a) Stress as deduced from curvature measurements during growth. The numbers indicate complete layer filling as determined from MEED measurements in (c). (b) Calculated slope of the stress curve (a) shows pronounced monolayer oscillations. The continuous curve serves as a guide to the eye. (c) Intensity of the specular reflected electron beam during Co deposition. Extrapolation back to the beginning of growth identifies the maximum intensity for filled layers.

study has identified some concerns regarding the direct access to lattice-spacing oscillations from reflective high energy electron diffraction rod-spacing oscillations [25]. Therefore, a direct measurement of stress oscillations offers a new avenue for studying atomic relaxation in monolayers.

We present stress measurements during the epitaxial growth of Co monolayers on Cu(001). The stress induced by the Co layers is found to oscillate as a function of film thickness with a period of one atomic layer. We have combined the stress measurements with medium-energy electron diffraction (MEED) analysis of the film morphology and found maximum stress for filled layers. Atomic-scale simulations performed by means of the quasi-*ab initio* molecular dynamics method show that strain relaxation in Co islands causes this novel effect of stress oscillations [26]. The stress measurements indicate a reduction of the strain energy per atom by 1 meV for island coverage at partial layer filling, which is too small to induce the transition from two- to three-dimensional growth mode.

Stress changes and growth-induced roughness of the Co film were measured simultaneously during growth by the set-up shown in figure 1. Film roughness is monitored by measuring the intensity of a 3 keV electron beam after specular reflection from the sample surface.

A measurement of the Co-induced stress $\tau_F \times t_F$ during deposition is shown in figure 4(a). We see that the total stress in the film increases monotonically. After deposition of 6 ML Co the stress has increased by 3.6 N m^{-1}, which corresponds to an average film stress of 3.37 GPa. The main result of this work is that the stress curve in figure 4(a) shows periodic changes in

its slope. This is obvious from the plot of the slope in figure 4(b), where 1 ML period of the stress oscillations is apparent. Before we discuss a model, that ascribes this finding to stress relaxation in Co islands, we elucidate the important result of an almost bulk-like stress behaviour of Co monolayers, which is reflected by the average film stress of 3.37 GPa.

The different lattice constants of fcc-Co (3.55 Å) and Cu (3.61 Å) induce a lattice mismatch $\epsilon = 1.7\%$ for the pseudomorphic growth regime. A film stress of $\tau_F = Y'_F\epsilon = 3.23$ GPa is calculated from continuum elasticity, with the biaxial modulus of fcc-Co $Y'_F = 190$ GPa.

This close agreement between the measured average film stress of 3.37 GPa and the continuum elasticity value of 3.23 GPa, indicates the dominant role of film strain for the measured stress. This result cannot be taken for granted as several previous experimental studies have found complete failures of stress–strain models in monolayers [17, 27–30]. In contrast to these studies, we suggest that for Co growth on Cu the charge transfer between the film and substrate, which has been proposed as an important factor in surface-stress changes [8], seems to be of minor relevance, making the film strain the decisive source of the measured stress.

Pronounced periodic changes in the slope of the stress curve are shown in figure 4(b). Minima of the slope are observed for less-than-half-filled layers, and maxima of the slope are observed for the almost filled layers. This phase relation between stress and layer filling is evident from the MEED and curvature data taken simultaneously. The stress oscillation shown in figure 4(b) indicate that, starting from a filled layer, the increase in stress due to newly arrived Co atoms is less than average ($\approx$0.6 N m^{-1}) for the first half monolayer and higher than average for the second half of the monolayer. This new and unexpected result is explained in the following text.

For $t_F > 2$ ML Co-growth on Cu(001) is a prototype of layer-by-layer growth [31], and we concentrate on this thickness regime. The smaller increase in the integrated film stress for less-than-half-filled layers relative to filled layers is correlated by the existence of many Co islands on top of the completed Co layer. Our *in situ* MEED analysis indicates maximum film roughness for half-filled layers. Therefore, one might wonder, why does the system proceed with a layer-by-layer growth, although this will lead to a larger elastic-energy content of the film? The low magnitude of the elastic energy offers an answer.

The elastic-energy density of the biaxially stressed Co film is calculated within continuum elasticity as 4.3 meV per Co atom. The application of continuum elasticity to the filled layer is physically justified by the validity of the stress–strain relation discussed above. The elastic-energy content of the fully strained Co layer is roughly two orders of magnitude smaller than the energy scale which governs alloy formation and surface diffusion [32–35] and it is therefore not sufficient in magnitude to induce island growth.

Our calculations reveal considerable bond-length variations for both island and substrate atoms, as shown in figures 5(a) and (b), respectively. The atomic positions in the Co island correspond to a reduced strain as compared to the pseudomorphic growth value (dashed line). Near the island edge, the bond lengths differ significantly for island atoms and atoms in the filled Co layer underneath: all Co island atoms show some strain relaxation, but atoms of the layer underneath near the island edge have a larger bond length as compared to the pseudomorphic value. Our stress calculations identify this structural relaxation as the origin of the stress oscillations.

In conclusion, we have found stress oscillations during the epitaxial growth of Co on Cu(001) with a period of 1 ML. Stress for filled layers of 3.37 GPa is followed by a reduced stress for less-than-half-filled layers. Our experiments and atomic-scale calculations ascribe the stress variation to the relaxation of epitaxial mesoscopic misfit strain in the islands. The stress measurements indicate an elastic energy per Co atom of 4.3 meV for filled layers, which

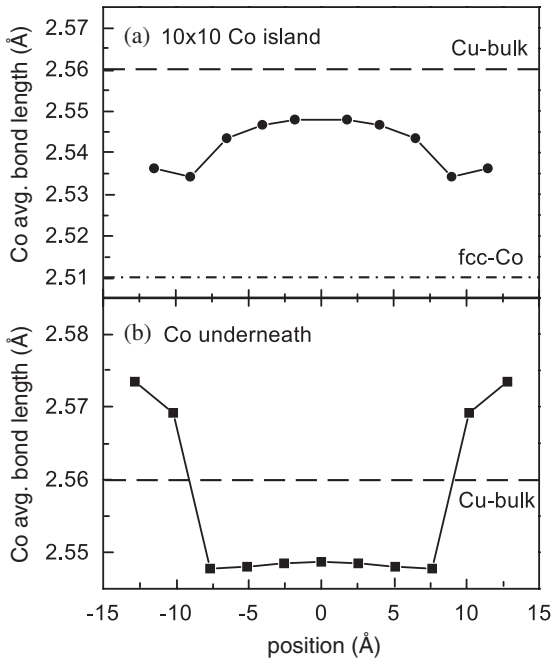

Figure 5. Calculated atomic distances in an island of 10 × 10 Co atoms (a) and in the filled Co layer underneath (b). (a) Co atoms are relaxed to give a Co–Co bond length considerably smaller than the pseudomorphic growth value (dashed line: Cu-bulk). (b) The Co atoms underneath have a larger bond length relative to the pseudomorphic growth value (dashed line) at the edge of the island. In the middle region, a compressed bond length is calculated.

is reduced to 3.3 meV for Co atoms in the top two layers of the island structure. The small magnitude of this energy variation indicates the dominant role of other energy contributions which lead to layer-by-layer growth in spite of the maximum strain energy in filled layers.

5. Magnetoelastic properties of ferromagnetic monolayers

An exciting aspect of the study of the physical properties of monolayers is that strain states are accessible in epitaxial films, that cannot be achieved in bulk samples. Even with high-strength materials, strain in excess of 1 the elasticity limits, and defects are formed. In epitaxial monolayers however, strains of several percent are measured and strongly modified physical properties are to be expected. The effect of strain on the modified magnetostrictive behaviour of monolayers is discussed as one example.

Magnetostriction, the change of the dimensions of a sample upon magnetization [36], is a term which should be limited to bulk samples. There, the sample is free to strain upon magnetization, whereas a film is not. For a film, magnetostrictive stresses are induced, and the amount of resulting strain depends on the stiffness of the substrate. The underlying physical principle is the strain dependence of the magnetic anisotropy, which is expressed by the magnetoelastic coupling coefficients B_i. They contribute to the energy density of the film via a term proportional to the strain ϵ, $B_i\epsilon$, and thus magnetoelastic stress B_i, or magnetostrictive stress for simplicity, is the driving force for magnetostriction [14]. These stresses induce a biaxial curvature of the substrate, as illustrated in figure 6.

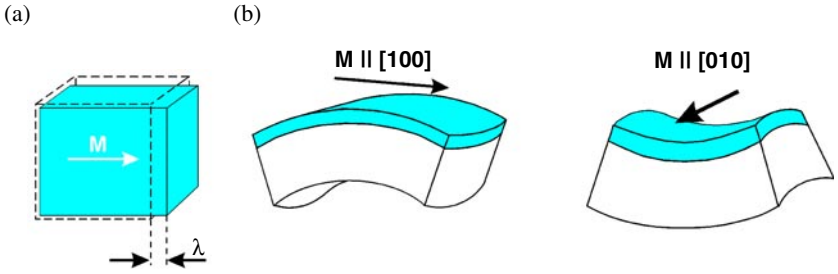

Figure 6. Schematic of magnetostrictive stress measurements. (a) Bulk samples show a strain λ upon magnetization M. (b) Films cannot expand freely as they are bonded to the substrate. Instead a magnetostrictive stress is created upon magnetization. The resulting curvature depends on the stiffness of the substrate and on the magnetization direction. Reorientation of the film magnetization from a direction along the sample length to the sample width induces a biaxial curvature change which is measured to extract the effective magnetoelastic-coupling coefficients.

(This figure is in colour only in the electronic version)

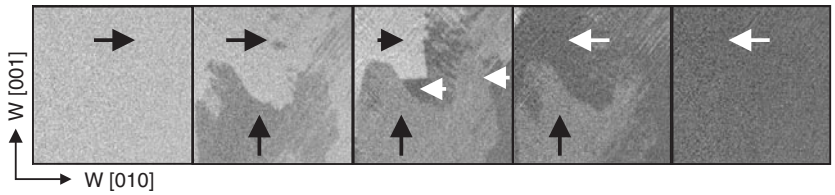

Figure 7. Kerr microscopy of the horizontal magnetization reversal in a 10 nm Co film on W(001). Image size is 2 mm × 2 mm. The arrows indicate the magnetization direction, which is displayed in a grey scale. The horizontal magnetic field was increased by 5 Oe for each image from left to right. Note that the inner images indicate a magnetization reversal with vertically magnetized domains. The appearance of both vertical *and* horizontal domains induces a magnetostrictive stress, as discussed in the text.

As in the case of epitaxial film stress, curvature analysis is employed to measure the change in curvature upon magnetization reversal, and the corresponding magnetoelastic coupling coefficients B_i, or combinations of these, are derived. We refer to [37] and references therein for both a detailed description of magnetoelastic coupling for different symmetries and for the curvature analysis.

Here, we concentrate on one aspect of these magnetoelastic stress measurements, which is the issue of the contribution of domains with different magnetization directions to the curvature signal. To measure the magnetoelastic-coupling coefficients, one has to switch the magnetization direction between two non-colinear directions. A simple reversal of the magnetization direction from left to right, from up to down is not sufficient, due to the quadratic dependence of the magnetoelastic coupling on the magnetization direction. Therefore, one has to employ in general magnetic fields along two perpendicular directions to measure the magnetoelastic-coupling coefficients properly, as shown in the following text.

As an example we discuss the magnetoelastic stress in a Co film on W(001) [38], which has an easy axis of magnetization within the sample plane, along the W⟨001⟩ directions. Kerr microscopy [39] is employed to image the domain orientation with the longitudinal magneto-optical Kerr effect (MOKE) during an in-plane reversal of the magnetization. The sequence of Kerr images is shown in figure 7. Here, the horizontal field was increased in steps of 5 Oe to induce a switching in the magnetization direction. The inner images reveal that during

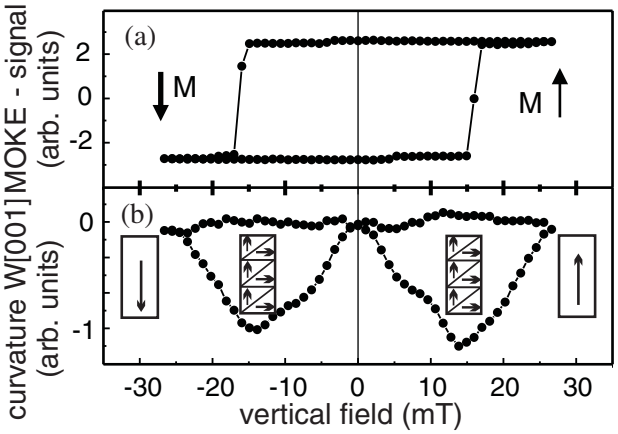

Figure 8. Simultaneous measurement of the transversal MOKE signal (a) and of the sample curvature along W[001] (b). During the magnetization reversal a negative curvature indicates compressive magnetoelastic stress, which is caused by the occurrence of horizontally *and* vertically magnetized domains, as indicated by the inset.

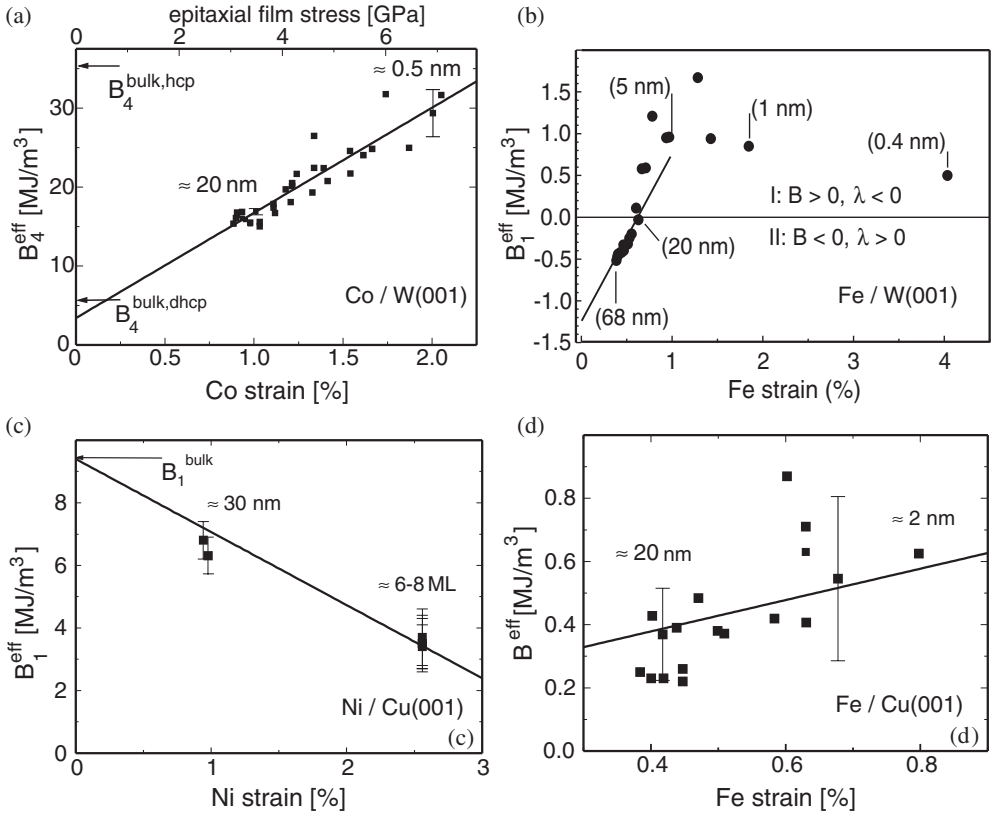

Figure 9. Effective magnetoelastic coupling coefficients as a function of film strain. (a) B_4^{eff} of Co on W(001), (b) B_1^{eff} of Fe on W(001), (c) B_1^{eff} of Ni on Cu (001), and (d) B^{eff} of Fe on Cu(001). Due to the epitaxial orientation, a combination of B_1^{eff} and B_2^{eff} is measured for Fe on Cu(001), see text. In all cases a linear relation between the effective coupling constant B and the film strain gives a fair description. For Fe on W(001) this linear relation holds up to a strain of 1%, as discussed in the text.

magnetization reversal domains with vertical magnetization direction are formed. However, these images reveal, that only a fraction of the surface was magnetized along the vertical direction.

We demonstrate in figure 8, how the simultaneous occurrence of domains with perpendicular magnetization directions leads to a sample curvature. However, this curvature is a factor of almost 4 smaller than that measured for a magnetization reversal with a constant vertical magnetic field present. A small constant vertical field ensures that the whole films switches to the vertical magnetization direction upon magnetization reversal, and the full magnetoelastic stress is measured [40]. Magnetization states with subsequent occurrence of two single domains with perpendicular magnetization directions have been produced for the following measurements of the magnetoelastic-coupling coefficients.

We used the cantilever bending technique to measure the effective magnetoelastic-coupling coefficients in epitaxial Fe [14, 41], Co [38] and Ni [41] films. We find that in all cases the measured coupling coefficients deviate substantially from the respective bulk values, for a 20 nm Fe film we even found a change of sign of B_1. The combined measurements of both film stress during film growth and magnetoelastic stress revealed the decisive role of film strain for the modified magnetoelastic properties of the epitaxially strained films. In figure 9 we present the results for B_i, plotted versus film strain, as deduced from the stress measurements. The epitaxial order of the films leads to the measurement of the following coefficients: (a) B_4 of hcp Co [38], (b) B_1 of bcc Fe [14], (c) B_1 of fcc Ni [41], and in (d) $(3B_1 + B_2)/4$ of bcc Fe [41]. A linear fit to the data is indicated by a straight line, which indicates linear dependence of the magnetoelastic coupling on film strain. This linear correlation between epitaxial strain and effective magnetoelastic coupling gives a fair description of the experimental data. Only for Fe on W(001), see figure 9(b), the deviation of the experimental data from the straight line indicates the severe limitations of the applied simple strain correction. The origin of this deviation for strain in excess of 1% remains to be clarified [14, 42].

These measurements indicate the important modification of magnetic anisotropy by film strain, which cannot be deduced properly by applying bulk magnetoelastic-coupling coefficients. Recent *ab initio* calculations also identified the decisive role of strain for the peculiar magnetoelastic behaviour of epitaxially strained films [42–45]. Future measurements of the magnetoelastic coupling of nanometre-scale alloy films are very important for the application of these films in magnetoelectronic devices and are currently underway.

References

[1] Hoffman R 1966 *Phys. Thin Films* **3** 211
[2] Kinosita K 1972 *Thin Solid Films* **12** 17
[3] Doerner M F and Nix W 1988 *CRC Crit. Rev. Solid State Mater. Sci.* **14** 225
[4] Nix W 1989 *Metall. Trans.* A **20A** 2217
[5] Abermann R 1990 *Vacuum* **41** 1279
[6] Koch R 1994 *J. Phys.: Condens. Matter* **6** 9519
[7] Daughton J, Pohm A, Fayfield R and Smith C 1999 *J. Phys. D: Appl. Phys.* **32** R169
[8] Feibelman P 1997 *Phys. Rev.* B **56** 2175
[9] Batirev I, Hergert W, Rennert P, Stepanyuk V, Oguchi T, Katsnelson A, Leiro J and Lee K 1998 *Surf. Sci.* **417** 151
[10] Qian X, Wagner F, Petersen M and Hübner W 2000 *J. Magn. Magn. Mater.* **213** 12
[11] Stepanyuk V, Bazhanov D and Hergert W 2000 *Phys. Rev.* B **62** 4257
[12] Stepanyuk V, Bazhanov D, Baranov A, Hergert W, Dederichs P and Kirschner J 2000 *Phys. Rev.* B **62** 15 398
[13] Marcus P, Qian X and Hübner W 2000 *J. Phys.: Condens. Matter* **12** 5541
[14] Sander D 1999 *Rep. Prog. Phys.* **62** 809
[15] Marcus P 1996 *Surf. Sci.* **366** 219

[16] Marcus P 1997 *J. Magn. Magn. Mater.* **168** 18
[17] Ibach H 1997 *Surf. Sci. Rep.* **29** 193
[18] Dahmen K, Lehwald S and Ibach H 2000 *Surf. Sci.* **446** 161
[19] He L and Lim C 2001 *Surf. Sci.* **478** 203
[20] Dahmen K, Ibach H and Sander D 2001 *J. Magn. Magn. Mater.* **231** 74
[21] Nye J F 1985 *Physical Properties of Crystals* (Oxford: Oxford University Press)
[22] Massies J and Grandjean N 1993 *Phys. Rev. Lett.* **71** 1411
[23] Fassbender J, May U, Schirmer B, Jungblut R, Hillebrands B and Güntherodt G 1995 *Phys. Rev. Lett.* **75** 4476
[24] Turban P, Hennet L and Andrieu S 2000 *Surf. Sci.* **446** 241
[25] Müller P, Turban P, Lapena L and Andrieu S 2001 *Surf. Sci.* **488** 52
[26] Sander D, Ouazi S, Bazhanov D, Stepanyuk V and Kirschner J 2001 unpublished
[27] Brandt O, Ploog K, Bierwolf R and Hohenstein M 1992 *Phys. Rev. Lett.* **68** 1339
[28] Grossmann A, Erley W, Hannon J B and Ibach H 1996 *Phys. Rev. Lett.* **77** 127
[29] Sander D, Schmidthals C, Enders A and Kirschner J 1998 *Phys. Rev.* B **57** 1406
[30] Sander D, Enders A and Kirschner J 1999 *Europhys. Lett.* **45** 208
[31] Schmid A and Kirschner J 1992 *Ultramicroscopy* **42–4** 483
[32] Nouvertné F, May U, Bammig M, Rampe A, Korte U, Güntherodt G, Pentcheva R and Scheffler M 1999 *Phys. Rev.* B **60** 14 382
[33] Saúl A and Weissmann M 1999 *Phys. Rev.* B **60** 4982
[34] Pentcheva R and Scheffler M 2000 *Phys. Rev.* B **61** 2211
[35] Stepanyuk V, Bazhanov D, Hergert W and Kirschner J 2001 *Phys. Rev.* B **63** 153406
[36] Kittel C 1949 *Rev. Mod. Phys.* **21** 541
[37] Dahmen K, Ibach H and Sander D 2001 *J. Magn. Magn. Mater.* **231** 74
[38] Gutjahr-Löser T, Sander D and Kirschner J 2000 *J. Magn. Magn. Mater.* **220** L1
[39] Giergiel J and Kirschner J 1996 *Rev. Sci. Instrum.* **67** 2937
[40] Sander D, Skomski R, Enders A, Schmidthals C and Kirschner J 1998 *J. Phys. D: Appl. Phys.* **31** 663
[41] Gutjahr-Löser T, Sander D and Kirschner J 2000 *J. Appl. Phys.* **87** 5920
[42] Komelj M and Fähnle M 2000 *J. Magn. Magn. Mater.* **220** L8
[43] Fähnle M and Komelj M 2000 *J. Magn. Magn. Mater.* **220** L13
[44] Komelj M and Fähnle M 2000 *J. Magn. Magn. Mater.* **222** L245
[45] Komelj M and Fähnle M 2001 *J. Magn. Magn. Mater.* **224** L1